

ENERGY INJECTION EPISODES IN GAMMA RAY BURSTS: THE LIGHT CURVES AND POLARIZATION PROPERTIES OF GRB 021004¹

G. BJÖRNSSON, E. H. GUDMUNDSSON, G. JÓHANNESSON²

Draft version June 26, 2018

ABSTRACT

Several GRB afterglow light curves deviate strongly from the power law decay observed in most bursts. We show that these variations can be accounted for by including refreshed shocks in the standard fireball model previously used to interpret the overall afterglow behavior. As an example we consider GRB 021004 that exhibited strong light curve variations and has a reasonably well time-resolved polarimetry. We show that the light curves in the *R*-band, X-rays and in the radio can be accounted for by four energy injection episodes in addition to the initial event. The polarization variations are shown to be a consequence of the injections.

Subject headings: gamma rays: bursts — gamma rays: theory — polarization

1. INTRODUCTION

A long-duration gamma-ray burst (GRB) is now generally believed to occur following the core collapse of a massive star (Woosley 1993; Stanek et al. 2003; Hjorth et al. 2003). Following the collapse, the released energy pierces a hole through the star along its rotation axis, sweeps up and shocks the surrounding interstellar medium and produces a long-lived afterglow emission. According to the standard fireball model (Mészáros 2002; Zhang & Mészáros 2003; Piran 2004), the expanding fireball slows down as it sweeps up more and more ambient material and decays in brightness.

The standard fireball model (SFM) predicts that the afterglow light curves should be power laws in time, with a break due either to one of the characteristic frequencies of synchrotron radiation moving through the observing band (e.g. Sari et al. 1998) or because of the outflow being collimated (Rhoads 1999). The former would only give rise to a modest steepening, while in the latter case it can be substantial in addition to being achromatic. In most cases where a break has been observed, the steepening is substantial and achromatic in the optical domain and the latter explanation appears to be the appropriate one.

For the first GRB afterglow light curves observed, the SFM provided adequate interpretation of the data. In recent years, several well observed afterglows have shown strong deviation from smooth power-laws, e.g. GRB 011211 (Jakobsson et al. 2004), GRB 021004 (Fox et al. 2003; Holland et al. 2003), and GRB 030329 (Price et al. 2003; Matheson et al. 2003b; Lipkin et al. 2004). Bursts like GRB 000301C, GRB 020813 and GRB 010222 also deviate from the standard behavior as their initial light curve decay rate was slower than can be easily accommodated within the model. In these cases, a continuous energy injection may explain the slow decay as has been suggested for GRB 010222 (Björnsson et al. 2002).

For light curves showing 'bumps' and 'wiggles' during the first few days, as e.g. GRB 021004, it has been suggested that these might arise when the fireball encounters density irregularities in the ambient medium (Lazzati et al. 2002;

Heyl & Perna 2003; Nakar et al. 2003). Higher density regions would cause brightening episodes, while a rarification immediately following the higher density appears necessary to get the light curve decay 'back on track'. Fox et al. (2003) suggested that the light curve variability of GRB 021004 may be due to refreshed shocks. Recently, it has been claimed that such models can be rejected as they are unable to explain simultaneously the bumpy light curves and the polarization as the latter would not be affected by the freshly injected energy (Lazzati et al. 2003, hereafter L03).

In this Letter we show, contrary to the conclusions of L03, that several energy injection episodes may in fact explain the afterglow light curve re-brightenings of bursts like GRB 021004, each injection contributing to the light curve as it catches up with the previously expanding shock front (see also Granot et al. 2003, for a similar conclusion on GRB 030329). We consider injections in the SFM and apply our model to GRB 021004. We show that not only are the light curves readily accounted for, but also that its polarization properties follow directly from the model. Detailed account of this work as well as application to other bursts will be presented elsewhere (Jóhannesson et al. in preparation).

2. ENERGY INJECTION

For a general review of the SFM we refer the reader to Mészáros (2002), Zhang & Mészáros (2003) and Piran (2004). The basic idea behind the model is the self-similar relativistic shock solution of Blandford & McKee (1976), where it is assumed that energy is released instantaneously at the onset of the burst. It is, however, both natural and expected that the energy release may be either continuous or episodic (Rees & Mészáros 1998; Kumar & Piran 2000; Sari & Mészáros 2000).

We extend the SFM as suggested by Rees & Mészáros (1998) by applying energy and momentum conservation, as in Rhoads (1999), to both discrete and continuous energy injections although only discrete injections will be considered here. We assume that several discrete shells are injected simultaneously with different Lorentz factors. The shell with the highest Lorentz factor, Γ_0 , drives the initial evolution of the afterglow. Once it has decelerated to a value lower than the Lorentz factor of the next shell, they will collide with a delay corresponding to the time it takes the second shell to reach the first. The collision is assumed to be instantaneous and its dynamics is neglected as is any anisotropy that may results

¹ Some of the radio data referred to in this paper were drawn from the GRB Large Program at the VLA, <http://www.vla.nrao.edu/astro/prop/largeprop/>. NRAO is a facility of the National Science Foundation operated under cooperative agreement by Associated Universities, Inc.

² Science Institute, University of Iceland, Dunhaga 3, IS-107 Reykjavik, Iceland, e-mail: gulli, einar, gudlaugu@raunvis.hi.is

from the shell interactions. In afterglow interpretations, the delay is fixed by the start of a brightening episode. The energy of the shell is determined by the observed increase in flux level. Similar results can be achieved with a continuous energy injection as discussed by Panaitescu, Mészáros & Rees (1998), but requires a very steep energy injection profile and in some cases even a varying electron energy index, p .

In calculating light curves and spectra, we assume that the radiation is of synchrotron origin, and we consider the local synchrotron spectra at each point in the outflow to consist of power law segments, smoothly joined at the characteristic frequencies (Granot & Sari 2002). We integrate over a thin shell at the equal arrival time surface. Each shell element is assumed to be locally homogeneous, its thickness being determined by the jump conditions across the shock (Blandford & McKee 1976) and the conservation of particles. We can therefore consider general density profiles, for example a constant density environment, a wind or various density irregularities.

We calculate the instantaneous fireball polarization as in Rossi et al. (2004). We assume a random magnetic field compressed by the blast-wave, thereby introducing some alignment perpendicular to the compressed direction (Laing 1980). We evaluate at a given observer time the contribution of each surface element of the equal arrival time surface to the Stokes parameters $dU = P(\theta)dL\cos(2\phi)$, and $dQ = P(\theta)dL\sin(2\phi)$, with the angular dependence of the polarization given by $P(\theta) = P_0 \sin^2 \theta' / (1 + \cos^2 \theta')$ (Laing 1980). Here, θ' is the angle from the line of sight in the comoving frame and dL is the local luminosity. In the optical range for most of the fireball evolution, the maximum degree of polarization is taken to be $P_0 = (p+1)/(p+7/3) \approx 70\%$ for $p = 2.2$ (see Rybicki & Lightman 1979, for details). For a measurable polarization to occur, the line of sight to the observer has to be off the outflow symmetry axis (Ghisellini & Lazzati 1999; Sari 1999). As in Ghisellini & Lazzati (1999), we find that for an instantaneous energy release, the polarization light curve has two extrema, bracketing the time when $\theta \approx 1/\Gamma$. At approximately that time the polarization angle rotates by 90° (Ghisellini & Lazzati 1999; Sari 1999; Granot & Königl 2003). It is important to note that the maximum degree of polarization and time of change of the polarization angle depend strongly on the viewing angle. The polarization evolution depends mostly on the evolution of Γ , but is also affected by the evolution of the jet opening angle. Rossi et al. (2004) have shown that the larger the lateral velocity, the lower the polarization. We assume the sideways expansion is given by the comoving sound speed, $c_s = c/\sqrt{3}$. Recent work has shown that the lateral expansion may in fact be slower (Granot et al. 2001), but we adopt this assumption to highlight the effects of the energy injections.

The number of model parameters can be quite large if there are many brightenings. The global parameters: initial energy, E_0 , Lorentz factor, Γ_0 , half-opening angle, θ_0 , ambient density, n_0 (or density profile), relative energy density in electrons, ϵ_e , and magnetic field, ϵ_B , and electron index, p , are determined, as in the SFM, from the initial afterglow evolution and the total flux level (using the burst redshift). All episode parameters are fixed by the observed time of brightenings and the increase in flux levels. As discussed by Zhang & Mészáros (2002) (hereafter ZM02), only the energy ratios and the relative velocities are relevant as long as the relativistic phase lasts, and therefore absolute shell energies and

Lorentz factors are not needed. If polarimetry is available this may be the most reliable way to determine the so called jet break time as the polarization angle is predicted to change by 90° at that time. Determining the break time from a broken power-law fit to the optical light curve can lead to an erroneous result if the light curve is not smooth, as e.g. in the case of GRB 021004. In addition, for the interpretation to be consistent, the polarization levels predicted by the model should agree with those observed, once all parameters have been determined. Our code has been extensively tested and compared to other work. We have also compared the output with analytical results, and find good agreement in parameter ranges where the assumptions used in analytical work are valid.

The effects of a single injection episode can be described as follows: When a relativistic shell catches up with the slower shock front propagating into the ambient medium, it increases the Γ of the forward shock (ZM02), but the subsequent evolution of Γ continues with the same decay rate as before. Reverse shocks may be expected, but these are expected to be weak for mild energy injections (ZM02). The flux from the fireball increases, but as the energy addition is instantaneous the light curve decay will from then on also continue with the same rate as prior to the shell injection. The rise in flux will not be sharply defined in time as the flux is obtained by integration over the equal arrival time surface that smooths out the transition. The injected shell will thus result in a smooth bump in the light curve. The net result is that the light curve is 'shifted' upwards at the time of the injection, but retains its original decay rate behavior from then on, the rate being most strongly determined by p , and the density structure of the ambient medium (e.g. Panaitescu, Mészáros & Rees 1998). Each energy injection episode delays the decaying evolution of Γ , and causes it to increase temporarily. In addition, the emitting region of the relativistic outflow centered on the line of sight, temporarily brightens up and outshines the bright emitting ring-like region around the line of sight (see Waxman 1997; Panaitescu & Mészáros 1998; Granot et al. 1999, for a detailed discussion). As a result the flux will increase slowing the light curve decay (Kumar & Piran 2000). It is important to realize that contrary to earlier statements (L03), polarization will also be affected by the energy injection, as increasing Γ increases the flux, causes increased aberration, decreases the emitting surface area and thus decreases the degree of polarization compared to an unperturbed evolution. We will show examples of these effects in the next section. Additional injections can be viewed as superpositions of repeated single episodes with similar effects on the light curve.

3. GRB 021004

As an example, we consider GRB 021004. It showed strong light curve variations with a best fit light curve break time of 4.74 days (Holland et al. 2003). This break time was obtained by fitting a broken power law to the data and resulted in a rather large formal error. The afterglow also exhibited variable polarization levels and a 90° change in polarization angle at approximately 1.0 day (Rol et al. 2003). These two time estimates, if interpreted within the SFM, should be similar but are in this case inconsistent with each other.

We find that the light curves can be explained by 4 injection episodes, superimposed on the initial GRB event. We summarize the model parameters in Table 1, and show the model light curves in Fig. 1. We set $p = 2.2$, as theoretical studies suggest this to be a universal value (see Piran 2004, for a review and references). Using the burst redshift, $z = 2.335$ (e.g.

TABLE 1
MODEL PARAMETERS FOR GRB 021004

Parameter	Value
E_0	1.0
Γ_0	800
p	2.2
n_0	26.0
E_1	3.5
E_2	5.6
E_3	13.0
E_4	7.0

Initial half-opening angle is $\theta_0 = 1.4^\circ$, the line of sight angle is $\theta_v = 0.95\theta_0$, $\epsilon_e = 0.21$, and $\epsilon_B = 2 \cdot 10^{-4}$. n_0 is in units of cm^{-3} , E_0 is in units of 10^{50} ergs, and the four energy injection values, E_i , are relative to E_0 . The four injection times in the observer frame are approximately 1 h, 16 h, 42 h and 105 h.

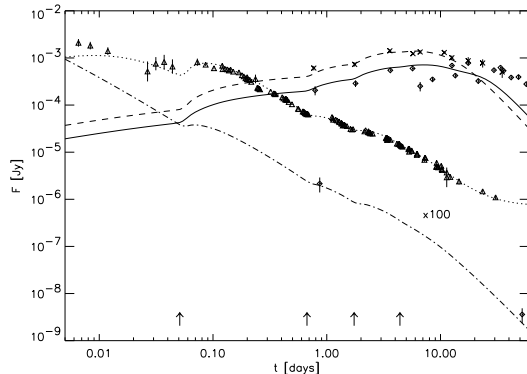


FIG. 1.— Light curves of GRB 021004: R -band (dotted), 8.46 GHz (solid), 22.5 GHz (dashed), and X-ray (multiplied by a factor of 100; dash-dotted). Variability in the optical light curve is obtained by imposing 4 energy injection episodes at times indicated by the arrows. Parameters were adjusted so that the model light curves would also go through the X-ray and radio light curves as well as the polarization data. A host galaxy of R -band magnitude 24 was added to the model optical light curve. R -band data is from Uemura et al. (2003); Pandey et al. (2003); Holland et al. (2003). X-ray data is from Sako & Harrison (2002a,b). Radio data is from Berger, Frail, & Kulkarni (2002); Frail & Berger (2002) and the GRB Large Program at the VLA (AK509)¹. Radio data hints at a 5th injection at 11-12 days.

Møller et al. 2002), E_0 , Γ_0 and n_0 , are determined by demanding that the model flux matches that observed in the same way as in the standard model. The bumps in the R -band light curve are then used to set the times and relative energies of the injection episodes. Other parameters, such as ϵ_e and ϵ_B , are then adjusted until the model agrees with the radio and X-ray data. Finally, the change in polarization angle to fix the opening angle of the jet, 1.4° . Recall that this depends on the rate of lateral expansion, here assumed to be constant.

All four injections are mild (ZM02), the relative Lorentz factor in all cases about 2. The relative energy of the first injection is 3.5, in subsequent episodes it is 1.24, 1.27 and about 0.3 of the total in the fourth episode. The peak flux from the reverse shocks is maximum for the first event, a factor of 30 higher than from the forward shock with the frequency at maximum reverse flux of about 2.5 GHz. No radio data is available at the time of the first injection. All subsequent reverse shocks have lower maximum fluxes and frequencies in the sub-GHz range. We therefore neglected the reverse shock contributions to the flux.

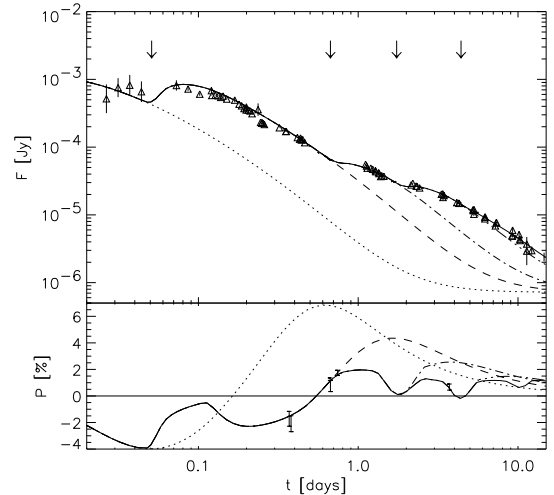


FIG. 2.— A segment of the R -band light curve of GRB 021004 (top panel). Effects of each of the energy injection events is shown. Dotted curve shows the theoretical afterglow model without additional energy injection. Dashed curve shows the effect of one injection event, dot-dashed two events, dash-triple-dotted three events and the solid curve shows the effect of all four injection events. Arrows indicate the injection times. Lower panel shows the corresponding polarization light curves. Note how each injection episode causes the polarization to deviate from the curve of unperturbed evolution. Polarimetry data is from Rol et al. (2003) and L03.

As seen in Fig. 1, the model is able to account for the light curves in all observed wavelength regions at all times, except for the first half hour or so when an initial reverse shock may be dominating the flux (Kobayashi & Zhang 2003; Panaitescu & Kumar 2004), and the radio data after about 20 days. A fifth injection may be able to account for the late radio data followed by a transition to a non-relativistic expansion regime at 50-60 days.

The intrinsic optical and X-ray spectral slopes are fixed by our choice of $p = 2.2$. At 1.4 days these are $\beta_{\text{opt}} = (p-1)/2 = 0.6$ and $\beta_X = p/2 = 1.1$. The former is within 2σ of the intrinsic (extinction corrected) spectral index, estimated in Holland et al. (2003), of $\beta_{UH} = 0.39 \pm 0.12$. Matheson et al. (2003a) find a steeper slope of the optical spectra but with a clear curvature, $\beta = 0.98 \pm 0.03$. Holland et al. (2003) also obtained an excellent fit to the 2–10 keV *Chandra* spectral index of 1.03 ± 0.06 , agreeing with the model prediction. In the 0.4–10 keV range and including absorption, they find $\beta_X = 0.94 \pm 0.03$. These results are consistent with those of Butler et al. (2003) and Sako & Harrison (2002a).

In Fig. 2 we plot the R -band and polarization light curves of GRB 021004. We show the effect of each injection episode separately as well as the combined result. With this interpretation, the estimate by Holland et al. (2003) of the late jet break time now has a simple explanation. The repeated energy injections slow the early light curve decay and delay the steepening until after the last injection. A broken power law thus underestimates the pre-break decay slope and overestimates the jet break time. The change in polarization angle should give a more reliable estimate of the break time.

As mentioned above, with only one energy release event, we recover the polarization behavior of Ghisellini & Lazzati (1999) with differences due to our more detailed fireball model (dotted curves). Adding one injection episode clearly shows the effects on the optical and polarization light curves

(dashed in fig. 2). At the time of injection the polarization level drops sharply and reaches a minimum just after maximum brightness in the light curve. In this particular burst, the first injection occurs before the jet break, and because the injection modifies the temporal evolution of Γ , it delays the jet break time compared to a single event, and hence also the 90° change in polarization angle. The break time, as defined by the change in polarization angle, is approximately at 0.6 days. This is just before the 2nd injection and therefore goes unnoticed in the light curves until after the last injection.

Including all four injections results in the polarization light curve shown in the lower panel in fig. 2 (solid). There, the effect of each injection episode is very clear. Depending on the strength of the injections, the polarization angle may change again, although at a very low polarization level (see local minimum at approximately 4 days). The correlation between the observed flux and polarization variations is in this interpretation seen to be directly rooted in the dynamics of the outflow.

4. DISCUSSION

We have also applied our code to a SFM modified with density variations in a homogeneous medium, but without energy injections. We modeled the variations with Gaussian profiles as in L03. The calculated flux is very sensitive to the number of radiating electrons and care must be taken in counting them. Only when we specifically introduced the shock profile of Blandford & McKee (1976), did we manage to get sufficient brightenings. A proper treatment of the effects of density variations, valid at all observer times and radial ranges of interest here, requires a numerical solution of the dynamical equations and a self consistent integration over the emitting region.

Nakar & Oren (2004) have interpreted the GRB 021004 optical data using the “patchy shell” model where the angular distribution of energy in the shock is inhomogeneous due to random fluctuations. Its application requires the angular energy distribution to be specified, but with suitable parameters the model is able to account for the general trends in the data.

A contribution to the polarization may originate in

the Galaxy or within the host. L03 conclude that for GRB 021004, the host contribution can be accounted for by using spectropolarimetric data, while the Galaxy may dominate at low polarization levels. However, the time variation of the polarization can only originate in the source.

It is natural to assume that the central source releases energy in several discrete events, essentially simultaneously. The total energy injected into the collimated outflow inferred from our model is about $3 \cdot 10^{51}$ erg. It is of the same order as estimated in other bursts after beaming correction (Frail et al. 2001). Applying beaming correction to the isotropic γ -ray energy estimated in Fox et al. (2003), we find that $1.5 \cdot 10^{49}$ ergs were emitted in γ -rays. We remind the reader that the narrow opening angle inferred from our modeling is a consequence of assuming a constant lateral expansion velocity. In this interpretation, most of the electromagnetic energy output in GRB 021004 was emitted at longer wavelengths.

In addition to GRB 021004, we have considered other burst with highly variable light curves, including GRB 970508 and GRB 030329. Most cases considered so far can be accounted for by discrete energy injections, with GRB 030329 a possible exception. This work will be discussed separately.

The self similar solution is based on the assumption of a uniform or a wind structured ambient medium. It may therefore be able to account for the overall behavior of the expanding shock, but one cannot expect it to be able to follow density variations in detail. For that a numerical solution of the dynamical equations is required. We conclude that refreshed shocks *can* in fact account for the observed variability both in the light curves and in the polarization properties of bursts. The strongest argument in favor of our interpretation is the fact that we are able to account for both broad band behavior as well as the polarimetry within a single model.

We thank the referee for a constructive report and P. Jakobson for helpful comments on the manuscript. This work was supported in part by the University of Iceland Research Fund and a special grant from the Icelandic Research Council.

REFERENCES

- Berger, E., Frail, D. A., & Kulkarni, S. R. 2002, GCN 1613
 Björnsson, G., Hjorth, J., Pedersen, K., & Fynbo, J. U. 2002, ApJ, 579, L59
 Blandford, R. D. & McKee, C. F. 1976, Physics of Fluids, 19, 1130
 Butler, N. R., Marshall, H. L., Ricker, G. R., Vanderspek, R. K., Ford, P. G., Crew, G. B., Lamb, D. Q., & Jernigan, J. G., 2003, ApJ, 597, 1010
 Fox, D. W., et al., 2003, Nature, 422, 284
 Frail, D. A., et al., 2001, ApJ, 562, L55
 Frail, D. A., & Berger, E. 2002, GCN 1574
 Ghisellini, G. & Lazzati, D. 1999, MNRAS, 309, L7
 Granot, J., Piran, T., & Sari, R. 1999, ApJ, 513, 679
 Granot, J., et al., 2001, in GRBs in the Afterglow Era, ed. E. Costa, F. Frontera, & J. Hjorth, (Berlin:Springer), 312
 Granot, J. & Sari, R. 2002, ApJ, 568, 820
 Granot, J. & Königl, A. 2003, ApJ, 594, L83
 Granot, J., Nakar, E., & Piran, T. 2003, Nature, 426, 138
 Heyl, J. S. & Perna, R. 2003, ApJ, 586, L13
 Hjorth, J., et al., 2003, Nature, 423, 847
 Holland, S. T., et al., 2003, AJ, 125, 2291
 Jakobsson, P., et al., 2004, New Astronomy, 9, 435
 Kobayashi, S. & Zhang, B. 2003, ApJ, 582, L75
 Kumar, P. & Piran, T. 2000, ApJ, 532, 286
 Laing, R. A. 1980, MNRAS, 193, 439
 Lazzati, D., Rossi, E., Covino, S., Ghisellini, G., & Malesani, D. 2002, A&A, 396, L5
 Lazzati, D., et al., 2003, A&A, 410, 823 (L03)
 Lipkin, Y. M., et al., 2004, ApJ, 606, 381
 Mészáros, P. 2002, ARA&A, 40, 137
 Matheson, T., et al., 2003a, ApJ, 582, L5
 Matheson, T., et al., 2003b, ApJ, 599, 394
 Møller, P., et al., 2002, A&A, 396, L21
 Nakar, E., Piran, T., & Granot, J. 2003, New Astronomy, 8, 495
 Nakar, E., & Oren, Y. 2003, ApJ, 602, L97
 Panaitescu, A. & Mészáros, P. 1998, ApJ, 493, L31
 Panaitescu, A., Mészáros, P. & Rees, M. J. 1998, ApJ, 503, 314
 Panaitescu, A. & Kumar, P. 2004, MNRAS, in press (astro-ph/0406027)
 Pandey, S. B., et al., 2003, BASI, 31, 19
 Piran, T. 2004, Rev. Mod. Phys., in press (astro-ph/0405503)
 Price, P. A., et al., 2003, Nature, 423, 844
 Rees, M. J. & Mészáros, P. 1998, ApJ, 496, L1
 Rhoads, J. E. 1999, ApJ, 525, 737
 Rol, E., et al., 2003, A&A, 405, L23
 Rossi, E. M., Lazzati, D., Salmonson, J. D., & Ghisellini, G. 2004, MNRAS, in press
 Rybicki, G. B. & Lightman, A. P. 1979, Radiative processes in astrophysics (New York, Wiley-Interscience, 1979. 393 p.)
 Sako, M. & Harrison, F. A. 2002a, GCN Circ. 1624
 Sako, M., & Harrison, F. A. 2002b, Circ. 1716
 Sari, R., Piran, T., & Narayan, R. 1998, ApJ, 497, L17
 Sari, R. 1999, ApJ, 524, L43
 Sari, R. & Mészáros, P. 2000, ApJ, 535, L33
 Stanek, K. Z., et al., 2003, ApJ, 591, L17
 Uemura, M., et al., 2003, PASJ, 55, L31
 Waxman, E. 1997, ApJ, 491, L19
 Woosley, S. E. 1993, ApJ, 405, 273
 Zhang, B. & Mészáros, P. 2002, ApJ, 566, 712 (ZM02)
 Zhang, B. & Mészáros, P. 2003, Int. J. Mod. Phys. A, 19, 2385